# Title: Inhibition of miR-199b-5p reduces pathological alterations in Osteoarthritis by targeting *Fzd6* and *Gcnt2*.

**Authors:** Tong Feng[1]†, Qi Zhang[1,2]†, Si-Hui Li[1], Shuan-hu Zhou[3,4], Xin Wang[5], Jun-Meng Wang[1], Fan-Rong Liang[1], Shu-Guang Yu[1,6]*, Qiao-Feng Wu[1, 6]*

**Affiliations:**

1 Acupuncture and Tuina College, Chengdu University of Traditional Chinese Medicine, Chengdu, Sichuan, 610075, China

2 Chongqing Hospital of Traditional Chinese Medicine, Chongqing, 400011, China

3 Department of Orthopedic Surgery, Brigham and Women's Hospital, Harvard Medical School, Boston, Massachusetts, 02115, USA

4 Harvard Stem Cell Institute, Harvard University, Cambridge, Massachusetts, 02138, USA

5 Departments of Neurosurgery, Brigham and Women's Hospital, Harvard Medical School, Boston, Massachusetts, 02115, USA

6 Acupuncture & Chronobiology Key Laboratory of Sichuan Province, Chengdu, Sichuan, 610075, China

*Corresponding authors.

Qiao-feng Wu: wuqiaofeng@cdutcm.edu.cn

ORCID: 0000-0002-8308-2843

Shu-guang Yu: ysg@cdutcm.edu.cn

ORCID：0000-0002-1413-8989

Address: No.37, Road Shi-Er-Qiao, Jinniu District, Chengdu, Sichuan, 610075, China

† These authors contributed equally to this manuscript.


## Abstract

Osteoarthritis (OA) is a degenerative disease with a high prevalence in the elderly population, but our understanding of its mechanisms remains incomplete. Analysis of serum exosomal small RNA sequencing data from clinical patients and gene expression data from OA patient serum and cartilage obtained from the GEO database revealed a common dysregulated miRNA, miRNA-199b-5p. In vitro cell experiments demonstrated that miRNA-199b-5p inhibits chondrocyte vitality and promotes extracellular matrix degradation. Conversely, inhibition of miRNA-199b-5p under inflammatory conditions exhibited protective effects against damage. Local viral injection of miRNA-199b-5p into mice induced a decrease in pain threshold and OA-like changes. In an OA model, inhibition of miRNA-199b-5p alleviated the pathological progression of OA. Furthermore, bioinformatics analysis and experimental validation identified *Gcnt2* and *Fzd6* as target genes of miRNA-199b-5p. Thus, these results indicated that miRNA-199b-5p/*Gcnt2* and *Fzd6* axis might be a novel therapeutic target for the treatment of OA.



**Keywords: Osteoarthritis; Extracellular matrix; miRNA-199b-5p; Animal**


## Introduction

Osteoarthritis (OA) is a degenerative disease characterized by the deterioration of articular cartilage and affecting all components of the joint, including the synovium, subchondral bone, and meniscus[1]. Knee OA (KOA) is the leading cause of disability and increased living costs among elderly patients[2]. Currently, the treatment options for osteoarthritis are limited to symptomatic relief and joint replacement. However, the insufficient relief of symptoms, potential medication

side effects, and the economic burden and complications associated with joint replacement surgeries have prompted the need to identify new, effective, and safe treatment methods and explore unknown targets for individuals with KOA[3].

Exosomes are extracellular vesicles that are distributed in body fluids such as serum and play a crucial biological role by delivering molecules such as MicroRNAs (miRNAs)[4]. They serve as vital carriers for intercellular communication and transfer of genetic information. MiRNAs are a class of non-coding RNAs ranging from 18 to 24 nucleotides in length, which exert inhibitory effects on the expression of target genes through interactions with mRNA. Studies have demonstrated that miRNAs play a crucial role as a pathogenic factor in osteoarthritis (OA). [5]. For instance, miR-199b-5p was found to contribute to the osteogenic differentiation of bone marrow stromal cells [6]; another miR-140 showed cartilage-specific expression, and its expression was significantly reduced in OA cartilage [7;8].recently, intra-articular injection of antisense oligonucleotides of miR-181a-5p produced chondroprotective effects in OA mice [9].

In this study, we initially screened miR-199b-5p as a potential key miRNA based on clinical data by detecting differentially expressed exosomal miRNAs. To elucidate the role and function of miR-199b-5p, we investigated its impact on chondrocytes, which are crucial pathogenic cells in KOA, and identified its molecular targets through in vitro experiments. Furthermore, we explored its role in vivo. Hence, this article not only identifies miR-199b-5p as a potential microtarget for KOA but also provides a potential strategy for future identification of new molecular drugs.

## Results

66 **Identification and enrichment analysis of differentially expressed miRNAs in serum exo-**
67 **somes**

68 To investigate the dysregulated miRNAs in serum exosomes of KOA patients, we extracted exo-
69 somal miRNAs from serum and performed sequencing. Serum samples from 15 patients with
70 KOA and 10 healthy subjects were collected (Supplementary Table 2). After extraction, the se-
71 rum exosomes were observed under transmission electron microscopy and nanoparticle tracking
72 analysis, revealing a diameter ranging from approximately 70 to 150 nm (Fig. S1A, B). Further-
73 more, the surface marker proteins CD9, CD63, and CD81 were found to be expressed on the ex-
74 osomes (Fig. S1C). Next, we performed sequencing of miRNAs in serum exosomes.

75 The results showed that 88 miRNAs were up-regulated and 89 miRNAs were downregulated in
76 KOA patients compared with the control group based on fold change > 1.5 and $p < 0.05$ (Fig.
77 1A, B). Afterwards, we performed bioinformatics Gene Ontology (GO) and Kyoto Encyclopedia
78 of Genes and Genomes (KEGG) analyses on these differentially expressed genes. Among the top
79 5 enriched results of up-regulated differentially expressed miRNAs, the CC (Cell, intracellular,
80 and cytoplasm) GO terms were notable. The MF (Translation activator activity, binding to ubiq-
81 uitin-conjugating enzymes, and possessing transferase activity) GO terms and BP (Cell differen-
82 tiation and the stabilization of mRNA through 3'-UTR mediation) GO terms were also significant
83 (Fig. 1C). The top 10 enriched KEGG pathways, PI3K-AKT signaling, Ras signaling, apoptosis,
84 and other types of O-glycan biosynthesis are considered to be of significant importance (Fig.
85 1D).The analysis of the top 5 down-regulated differential miRNAs reveals interesting findings.
86 the CC (Cell, intracellular) GO terms were particularly noteworthy. The MF (RNA polymerase II
87 transcription factor activity and sequence-specific DNA binding) GO terms, as well as the BP
88 (collagen-activated signaling pathway) GO terms, were also deemed significant (Fig. 1E). More-

over, the analysis of the top 10 enriched KEGG pathways revealed a strong association with the Hedgehog signaling pathway, pluripotency of stem cells, and glycosaminoglycan biosynthesis-keratan sulfate (Fig. 1F).

It is noteworthy that in the aforementioned results, both the up-regulated and down-regulated differential miRNA enrichment analyses are involved in processes related to cartilage synthesis, including O-glycan biosynthesis and glycosaminoglycan biosynthesis-keratan sulfate[10;11].

**Dysregulated serum exosomal miRNAs were found to be expressed in both serum and cartilage**

Subsequently, we aimed to investigate whether these dysregulated miRNAs in serum exosomes show differential expression in other affected sites or tissues of KOA. Leveraging the KOA patient cartilage and serum sequencing data available in the GEO database, we compared our dysregulated miRNA list with the datasets. Remarkably, we identified 169 miRNAs that exhibited differential expression in the serum of KOA patients (Fig. 2A), suggesting their involvement in the disease. Moreover, these miRNAs were also found to be expressed in KOA patient cartilage (Fig. 2B). This robust validation reinforces the reliability of our data. Consequently, we proceeded with further screening of differentially expressed genes.

**miRNA-199b-5p has been identified as a potential target molecule in KOA.**

Based on the P-value and exosomal expression, five miRNAs（hsa-mir-3168, hsa-mir-1296-5p, hsa-mir-15b-3p, hsa-mir-338-3p and hsa-mir-199b-5p) were selected to further research and validated in independent human samples by RT-qPCR (hsa-mir-199b-5p, $p < 0.01$; hsa-mir-3168,

111 $p$=0.33; hsa-mir-15b-3p, $p < 0.01$; hsa-mir-338-3p, $p$=0.20 and hsa-mir-1296-5p, $p < 0.01$) (Fig.
112 2C). To further explore the functional roles of these miRNAs, we established a mouse model of
113 KOA to evaluate their expression in the joints. Due to species limitations, we examined the ex-
114 pression of miR-199b-5p ($p$ <0.01), miR-15b-3p ($p$ <0.05) and miR-338-3p ($p$ <0.05) in joint
115 tissue samples (control *vs* M-0.5) (Fig. 2D). The results showed that only the expression trend of
116 miR-199b-5p was consistent between the clinical samples and the mouse arthritis model. There-
117 fore, we selected miR-199b-5p as the target for our subsequent research.

118

119 **miR-199b-5p mimic inhibits the cell viability and extracellular matrix (ECM) of chondro-**
120 **cytes and inhibitor restores LPS-induced chondrocytes damage.**

121 We first extracted mouse primary chondrocytes (Fig. 3A-C). In vitro experiments showed that
122 overexpression miR-199b-5p inhibited the viability of chondrocytes($p<0.01$) (Fig. 3D, Fig. S2).
123 we also find miR-199b-5p mimic increased the mRNA expressions of *MMP3* ($p$=0.09) and
124 *ADAMTS5* ($p<0.05$) and decreased the mRNA expression of *COL2A1*($p$=0.05), *AGGRECAN*
125 (p=0.20) and *SOX9* ($p$=0.22), which are often used as the biomarkers of chondrocytes ECM met-
126 abolic balance. In contrast, miR-199b-5p inhibitor decreased the mRNA expression of *MMP3*
127 ($p$<0.01) and *ADAMTS5* ($p$=0.11) and increased the mRNA expression of *COL2A1* ($p$=0.07),
128 *AGGRECAN* ($p$<0.01) and *SOX9* ($p$<0.01) (Fig. 3E–I). While some gene expression changes
129 may not be significant in statistic, but the modulation of miR-199b-5p expression has been ob-
130 served to exert an influence on the metabolic alterations of chondrocytes.

131 To explore the effect of miR-199b-5p under pathological conditions, an LPS-stimulated inflam-
132 mation chondrocyte cell model was established. We examined the effect of LPS at 5, 10, and 15

133 μg/ml on cell viability and found that cell viability was significantly decreased at 15
134 μg/ml($p$<0.001) (Fig. 2J). Next, we chose 15 μg/ml of LPS to establish a chondrocyte injury
135 model. The CCK-8 assay showed that miR-199b-5p inhibitor reversed the decrease of cell viabil-
136 ity caused by LPS ($p$<0.01) (Fig. 3K). Also, we revealed that LPS elevated *MMP3* ($p$<0.01) and
137 *ADAMTS5* ($p$<0.01) and decreased *COL2A1*($p$=0.06), *AGGRECAN* ($p$<0.01), and *SOX9* ($p$=0.13)
138 expression. In the presence of miR-199b-5p inhibitor, the changes in mRNA levels were re-
139 versed (Fig. 3L-P). These results suggest that miR-199b-5p overexpression reduces cell viability
140 and miR-199b-5p inhibition partly restores LPS-induced cell damage and ECM degradation.

141

142 **miR-199b-5p mimic induces inflammation in normal mice, and miR-199b-5p inhibitor alle-**
143 **viates symptoms in KOA mice.**

144 Now，we want to know the vivo role of miRNA-199b-5p. Firstly, we screened Adneovirus(AD)
145 and utilized High-AD as a vector to either overexpress or inhibit the expression of miR-199b-
146 5p(Fig. S3). Then, miR-199b-5p mimic was injected to the joint of mice (Fig. 4A) and a decrease
147 in pain threshold was found ($p$<0.01) (Fig. 4B). Four weeks later, serum *IFN-γ* ($p$<0.01) and
148 *TNF-α* ($p$<0.01) were also significantly increased (Fig. 4C, D). The cartilage of mice injected
149 with the miR-199b-5p mimic was slightly degraded ($p$=0.02) (Fig. 4E, F). Additionally, the ar-
150 ticular surface showed insect erosion (Fig. 4G). interestingly, the level of serum inflammation in
151 the miR-199b-5p inhibitor injection group was significantly decreased compared with the mimic
152 group (*IFN-γ*, $p$<0.01; *TNF-α*, $p$<0.01). These results indicated that intra-articular injection of
153 miR-199b-5p mimic induced inflammation response in mice.

154 Followingly, we established an MIA-induced KOA model to further investigate the role of miR-
155 199b-5p (Fig. S4). We observed a decrease in pain threshold in the model group, and recovery
156 was observed on the 10th day in the inhibitor group ($p<0.01$) (Fig. 5A, B). Joint tissues were tak-
157 en at the fourth week, and revealed that the expression of *IFN-γ* ($p<0.01$) and *TNF-α* ($p<0.01$)
158 decreased after inhibiting miRNA-199b-5p (Fig. 5C, D). Safranin-fast green staining of joints
159 showed recovery of articular cartilage degradation ($p<0.05$) (Fig. 5E, F), and the moth erosion of
160 the cartilage μCT was partly improved (Fig. 5G). These results proved that intra-articular injec-
161 tion of the miR-199b-5p inhibitor partly recovered pain, inflammation, and cartilage degenera-
162 tion in KOA mice.

163

164 **_Gcnt2_ and _Fzd6_ are two target genes of miR-199b-5p**

165 In order to investigate the underlying mechanism of miRNA-199b-5p, we utilized five widely
166 used miRNA target gene prediction tools, namely miRWalk, miRDB, TarBase, starbase, and
167 TargetScan, to identify potential target genes. Consequently, we identified six putative target
168 genes of miRNA-199b-5p (Fig. 6A). Bioinformatics analysis of the six possible target genes
169 showed that BP is in posttranscriptional regulation of gene expression and angiogenesis; CC is in
170 cytoplasmic vesicle and cell leading edge; and MF is in ubiquitin protein ligase binding and pro-
171 tein domain specific binding (Fig. 6B).

172 After Mimic infected cells, we found decreases expression in *Fzd6* (P<0.01), *Gcnt2* (P<0.01),
173 and *Caprin1* (P=0.024) in the chondrocytes (Fig. 6C). Conversely, after inhibitor infection, *Hif-*
174 *1α* (P=0.048), *Fzd6* (P<0.01) and *Gcnt2* (P<0.01) were increased and *Atg14* (P=0.042) increased
175 (Fig. 6D). Notably, we observed corresponding changes in the expression of *Fzd6* and *Gcnt2* up-
176 on miR-199b-5p overexpression and under-expression. Moreover, we predicted potential binding

177 sites for miRNA-199b-5p within the 3'-untranslated region (UTR) of these two target genes (Fig.
178 6E, F) and luciferase reporter assays confirmed that miR-199b-5p can bind to and suppress the
179 expression of both *Gcnt2* ($P < 0.01$) and *Fzd6* ($P < 0.01$) *via* their complementary sequences
180 (Fig. 6G, H). Furthermore, we found differential expression of *Fzd6* in both synovial tissue data
181 (GDS5401) and chondrocyte data (GDS3758) from KOA patients in the GEO profile (Fig. 6I, J).
182 Similarly, differential expression tendency of *Gcnt2* was observed in both the synovial tissue da-
183 ta (GDS5403) and GDS3758 from the same KOA patients (Fig. 6K, L). These findings provide
184 further validation to our results. Therefore, *Fzd6* and *Gcnt2* was confirmed as an important
185 downstream target for further research.
186

187 **Discussion**

188 In this study, we initially performed sequencing of serum exosomal miRNAs from clinical pa-
189 tients and identified 177 dysregulated miRNAs. Subsequently, through comparison with GEO
190 data, we found that 169 miRNAs were expressed in both KOA serum and cartilage. Following a
191 screening process, miR-199b-5p was selected for further experiments. In cell-based assays, we
192 discovered that miR-199b-5p can influence the viability of chondrocytes and cytokine-mediated
193 extracellular matrix metabolism. Moreover, in vitro experiments demonstrated that it can induce
194 inflammation and abnormal pain threshold in normal mice. Importantly, inhibition of miR-199b-
195 5p alleviated the pathological symptoms of KOA. Finally, these effects were achieved by target-
196 ing *Gcnt2* and *Fzd6* (Fig. 7). Thus, our findings demonstrated that miR-199b-5p might be a novel
197 potential therapeutic target for OA prevention and treatment.

198 miRNAs function as regulators of gene expression in biological processes by regulate mRNA
199 translation by specifically binding to the 3′UTRs of target mRNAs [12]. Exosomes are rich in

miRNAs, and various cells can secrete exosomes to target cells under physiological and pathological conditions, which function as delivery vehicles for miRNAs [13;14]. There is evidence suggesting that miRNAs can participate in various cellular processes (inflammation, cell viability, ECM dysregulation) and signaling pathways (Hedgehog signaling, PI3K-AKT signaling) relevant to OA[15;16]. Our differential miRNA enrichment analysis also strongly supports the correlation with these findings.

In cancer research, overexpression of miR-199b-5p can inhibit the proliferation, migration and invasion of prostate cancer cells in vitro and tumor growth and metastasis in vivo by targeting DDR1[17]. In addition, exogenous miR-199b-5p inhibited the growth of bone marrow mesenchymal stem cells (MSCs) and promoted the differentiation of bone MSCs into chondrocytes by targeting the *JAG1* pathway [18;19]. Our functional experiments showed that overexpression of miR-199b-5p reduced chondrocyte viability and the expression of anabolic factors such as COL2A1, AGGREGN, and SOX9. It also increased inflammation levels and decreased pain thresholds in control mice. Although no pathological changes were observed in the articular cartilage of control mice, a similar study demonstrated that pathological cartilage changes only occurred after six months in mice with miR-211 and miR-204 knockout[20]. Therefore, we speculate that the time of overexpression of miR-199b-5p in our experiment was too short, so it only caused inflammation and pain threshold response. To best of our knowledge, this is the initial investigation documenting the involvement of miR-199b-5p in KOA.

*Fzd6* is known to be up-regulated during the osteogenic differentiation of MSCs and can be regulated by miR-194-5p to activate the WNT signaling pathway, thereby promoting osteogenic differentiation of MSCs[21]. *Gcnt2* has been found to induce epithelial-mesenchymal transition and enhance migration and invasion of esophageal squamous cell carcinoma cells[22]. Our findings in-

223 dicate that miR-199b-5p plays a crucial role in KOA by targeting *Fzd6* and *Gcnt2*. Future re-
224 search should further explore the roles and mechanisms of *Fzd6* and *Gcnt2* in the context of
225 KOA.

226 This study also has some limitations. We initially detected serum exosomes miRNA and later
227 examined the miRNA through in vitro experiment and animal study. However, whether the
228 miRNAs targeting the joints have the same role as the serum exosome miRNAs or blood miRNA
229 has not been clear. We also performed direct intra-articular injection of adenoviral vectors. The
230 intra-articular injection can reduce the exposure of extra-articular tissue, thereby minimizing the
231 associated side effects and improving targeting. Besides, more in-vivo study such as gene
232 knockout mice study can be used in the future study.

233 In conclusion, we found that miR-199b-5p is elevated in osteoarthritis and may affect cell viabil-
234 ity and related cytokines by targeting *Gcnt2* and *Fzd6*. Overexpression of miR-199b-5p induced
235 OA-like pathological changes in normal mice and inhibiting miR-199b-5p alleviated symptoms
236 in KOA mice, suggesting it may be a target for treatment of OA. Through human clinical trials,
237 cell experiments, and animal models, we not only identified a new OA-related miR-199b-5p but
238 also examined the biological function of miR-199b-5p in OA.

## 239 MATERIALS AND METHODS

### 240 Human samples

241 Study participants were recruited from the Hospital of Chengdu University of Traditional Chi-
242 nese Medicine and the surrounding communities. The study was approved by the Ethics Review
243 Committee of the Hospital at Chengdu University of Traditional Chinese Medicine (2016KL-

244 017) and conformed to the ethical guidelines of the 1975 Declaration of Helsinki. Serum was
245 collected from all participants and serum samples were stored at -80°C.

246 **Human subjects**

247 Patients were enrolled if they fulfilled the following criteria: (1) diagnosed with KOA according
248 to the ACR; (2) age between 40 and 65 years; (3) agreed to cooperate with researchers in all re-
249 search procedures after enrollment; (4) provided with written informed consent. Patients with
250 any of the following conditions were excluded: (1) accompanied with other diseases such as
251 rheumatoid arthritis, bone tumors, and bone tuberculosis; (2) treated with intra-articular gluco-
252 corticoid or viscoelastic supplementation in the last six months; (3) knee replacement history; (4)
253 had complicated cardiovascular disease, diabetes, skin disease, and liver or kidney impairment;
254 (5) pregnant or breastfeeding women; (6) accompanied with mental and intellectual disabilities;
255 or (7) undergoing other clinical trials.

256 **Extraction and sequencing of serum exosome miRNAs**

257 Serum samples were filtered using 0.22 μM filters. Exosomes were isolated from the serum
258 sample using ExoQuick™ Exosome Precipitation Solution (System Biosciences) following the
259 manufacturer's instructions. Briefly, serum was thawed on ice and centrifuged at 4000 rpm for
260 15 min to remove any cells or cellular debris. Next, 50 μL ExoQuick Solution was added into the
261 200 μL serum sample and mixed thoroughly. The exosomes were suspended in PBS.

262 Exosomes were characterized by electron microscopy (Tecnai G2 Spirit 120KV, FEI), nanopar-
263 ticle tracking analysis (NTA) (NTA 3.2 Dev Build 3.2.16), and western blot analysis (for CD9,
264 CD63 and CD81). Sequencing was performed by single-end sequencing (1×150 bp) on Illumina
265 NextSeq 500. The libraries were sequenced on an Agilent 2100 Bioanalyzer platform. The
266 mirdeep2 software (https://www.mdc-berlin.de/content/mirdeep2-documentation) was used to

analyze the miRNA sequences and quantification. The heatmap was plotted based on the log2 (fold change), using Heatmap Illustrator software (Heml 1.0).

**Total RNA was isolated from human serum, cell and mice**

Chondrocytes using a kit (Yeasen,Shanghai, China) according to the manufacturer's instructions. Reverse transcription was performed using 1000 ng total RNA and a Prime Script RT Reagent Kit(Yeasen, Shanghai, China) or Prime Script RT Master Mix (Yeasen, Shanghai, China), which were used for miRNA and mRNA, respectively. For miRNA, the reactions were incubated at 42°C for 15 min followed by inactivation at 85°C for 5 s. qRT-PCR amplification was assessed in a CFX Connection Real-Time System (Bio-Rad) using the SYBR Premix Ex Taq II kit (Yeasen, Shanghai,China). The following cycling conditions were used: 95°C for 30 s, followed by 40 cycles of 95°C for 5 s and 60°C for 30 s. All reactions were performed in duplicate and normalized to the internal reference U6 for miRNA and GAPDH mRNA for mRNAs. The $2^{-\Delta\Delta CT}$ CT method was used to evaluate the relative mRNA/miRNA expression levels.

**RNA primer**

Primers are listed in Supplementary Table 1.

**Bioinformatics analysis**

GO analysis was performed, involving the biological process (BP), cellular component (CC), and molecular function (MF), using DAVID[23] (https://david.ncifcrf.gov/home.jsp).We used the miRNA target gene prediction websites miRDB[24](http://mirdb.org/), miR-Walk[25](http://mirwalk.umm.uni-heidelberg.de/), Starbase[26] (https://starbase. sysu.edu.cn/), DI-ANA-TarBase[27] (http://diana.imis.athena-innovation.gr/DianaTools/ index.php?r=tarbase/index), Targetscan[28] (https://www.targetscan.org/vert_72/). The target genes of mmu-miR-199b-5p were predicted, and the intersection of the target gene prediction list results of the five sites was taken.

290 The dysregulated miRNAs were compared to relevant published miRNA data from human KOA
291 patients. The dataset GSE105027 was obtained from serum samples of KOA patients, while
292 GSE175961 comprised sequencing data from KOA patient cartilage. Finally, we validated the
293 expression of the target genes Gcnt2 and Fzd6 in KOA patients using synovial data (GDS5401,
294 GDS5403) and cartilage data (GDS3758).

295 **Primary mouse chondrocyte culture**

296 Primary mouse cartilage was extracted following the protocol of Gosset et al.[29]. The cells were
297 cultured in F12 medium containing 10% fetal bovine serum and 1% penicillin-streptomycin at
298 37°C and a 5% $CO_2$. The medium was changed every three days, and cells were cultured to the
299 second passage for experiments. Cells were stimulated with LPS for 6 h before subsequent inves-
300 tigation.

301 **Animal model of KOA**

302 Animal experiments were performed using total of 108 8-week-old male C57BL/6 mice. The
303 protocol was approved by the Committee on the Ethics of Animal Experiments of Chengdu Uni-
304 versity of Traditional Chinese medicine (2019-04). After randomization, the KOA mouse model
305 was established by orthotopic injection of MIA (sigma) into the knee joint of mice. After the an-
306 imals were anesthetized with isoflurane in a small animal anesthesia machine, the right knee
307 joint of the mouse was shaved, the knee joint was flexed 90°, and 10 μL of MIA solution was
308 injected into the knee joint cavity using a 28G microsyringe. The syringe needle was slowly
309 withdrawn and the knee joint was gently moved. Before model establishment and at 3, 7, 10, 14,
310 21, and 28 days after model establishment. After the 3rd day and 14th day after the start of the
311 experiment, the experimental mice were injected with adenovirus (total volume 10μL) in the

knee joint, and the control mice were injected with empty adenovirus as a control (Hanbio tech, Shanghai, China)[30].

**Thermal pain threshold detection**

A pain threshold detection instrument was used to measure the latency of the right plantar leg raising reflex of mice under heat radiation. Three days before the experiment, mice were cut off from water for half a day and adapted to the environment for 1 h. A certain intensity of pyrogen was used to irradiate the plantar position of the mouse's right limb, and a machine was used to automatically record the time when the mouse moved the limb from thermal pain. The resting intensity of the thermal pain stimulator was set to 10%, and the maximum duration was set to 20 s to avoid prolonged heating and burning of skin. After the light source is aimed at the sole of the mouse, we observed the mouse in real time. If paw raising, paw licking, or paw retraction was observed, the irradiation was stopped and the irradiation time of the instrument was recorded. The right limb of each mouse was tested five times, with an interval of 10 min each time; outliers were eliminated, and the average value was calculated and included in the statistics[31].

**ELISA and μCT scanning**

Mice were sacrificed after four weeks, and serum was collected for ELISA assay (Jiangsu Jingmei Biotechnology Co., Ltd., Yancheng, China). The knee joint specimens of the right hindlimb of mice were scanned using a high-resolution micro-CT skysan1267 instrument (Bruker, Germany). The sample was removed from fixative and dried. The scanning parameters were as follows: voltage 55 KV, current 200 μA, and filter 0.25AL. After scanning, three-dimensional reconstruction was performed using NRecon1.7.4.2 software.

**Safranin Fast green staining**

334 Mouse knee joint staining was performed using the Safranin Fast Green Staining Kit (Servicebio
335 Biological Technology, Wuhan, China). The sample was examined under a microscope, and the
336 cartilage integrity was scored according to the OARSI grading system, in which the score ranged
337 from 0 to 6 points[32].

338 **Luciferase assay**

339 The wild-type (WT) and mutant-type (MUT) sequences (according to the predicted binding site)
340 were inserted into the pmiRGLO plasmid. HEK-293T cells were seeded in 6-well plates at 24 h
341 before transfection. GCNT2 and FZD6 3′UTR-wt and gcnt2 and fzd6 3′UTR-mut plasmids (500
342 ng) and 20 nmol miR-199b-3p and NC were co-transfected with Lipofectamine 3000 (Hanbio
343 Biotechnology, China) following the manufacturer's instructions. After 48h, firefly and Renilla
344 luciferase activities were calculated using the Promega Dual-Luciferase system following the
345 manufacturer's instructions (Hanbio tech, Shanghai, China). Firefly/Renilla luciferase was meas-
346 ured to evaluate relative luciferase activity.

347 **Statistical analysis**

348 Data are reported as the means ± SD. Normal distribution and homogeneity of variance of data
349 were first tested. Shapiro-Wilk test was used to verify data normality, while Levene's test or
350 Browne-Forsythe test was adopted for assessment of variance equality. Statistical analysis was
351 performed by unpaired two *t*-test and Tukey-corrected one-way analysis of variance (ANOVA)
352 for comparisons between groups. Tukey-corrected two-way ANOVA for the comparison of mice
353 thermal pain threshold data. $P < 0.05$ was considered statistically significant for all statistical
354 calculations. PRISM 8.0 (GraphPad Software, San Diego, CA, USA) was used for data analysis.

355

**Contributions:**

F.T., Z.Q., and Q.-F.W. designed the study.

F.T. performed most in vitro and in vivo experiments.

F.T. and J.-M.W. analyzed data.

Z.Q., Y.J. and S.-H.L. performed the miRNA sequencing and interpreted the data.

Z.Q., and Y.J collected and inspected human patient samples.

F.T. and Q.-F.W. wrote the manuscript.

All authors read and edited the manuscript.

F.-R.L., S.-G.Y., and Q.-F.W. supervised the study.

**Competing interests**

The authors declare that they have no known competing financial interests or personal relationships that could have appeared to influence the work reported in this paper

**Acknowledgements:**

This work was supported by the National Key R&D Program of China (No.2019YFC1709001); Innovation Team and Talents Cultivation Program of National Administration of Traditional Chinese Medicine (No. ZYYCXTD-D-202003); Fund of Science and Technology Department of Sichuan Province, China (No. 2021ZYD0081); and National Natural Science Foundation of China (No. 82174512, 81873383).

**Data Sharing Statement:**

All data are available in the main text or the supplementary materials.

**List of Supplementary Materials:**

Present a list of the Supplementary Materials in the following format.

Materials and Methods

Fig S1. Identification of exosome. (A) Transmission electron microscope scanning of isolated exosomes from the serum of participants. (B) The Nano sight particle analysis of isolated exosomes from the serum of participants. (C) The Western blot analysis of symbolic surface markers of isolated exosomes from the serum of participants.

Fig S2. Fluorescence of Adenovirus-Infected Chondrocytes.

Fig S3. Expression of adenovirus in mouse knee joint.

Fig S4. Establishment of KOA model in mice by injection of MIA. (A) Behavioral detection of animal thermal pain threshold. (B) Microscopic observation of the surface of the mouse knee joint. (C) Safranin-fast green staining and semiquantitative scoring of articular cartilage. (D) 3D reconstruction images of joints from μCT scans. $*P<0.05$, $**P<0.01$, $n=6$.

Table S1 Primers list

Table S2 Basic information of participants

**References**


1. Chen D, Shen J, Zhao W, et al. Osteoarthritis: toward a comprehensive understanding of pathological mechanism. *Bone research.* 2017;5:16044.
2. Hunter D, Bierma-Zeinstra S. Osteoarthritis. *Lancet (London, England).* 2019;393(10182):1745-1759.
3. Ito Y, Matsuzaki T, Ayabe F, et al. Both microRNA-455-5p and -3p repress hypoxia-inducible factor-2α expression and coordinately regulate cartilage homeostasis. *Nature communications.* 2021;12(1):4148.
4. Xu W, Yang Z, Lu N. From pathogenesis to clinical application: insights into exosomes as transfer vectors in cancer. *Journal of Experimental & Clinical Cancer Research : CR.* 2016;35(1):156.
5. Ali S, Peffers M, Ormseth M, Jurisica I, Kapoor M. The non-coding RNA interactome in joint health and disease. *Nature reviews Rheumatology.* 2021;17(11):692-705.
6. Zhao R, Li Y, Lin Z, et al. miR-199b-5p modulates BMSC osteogenesis via suppressing GSK-3β/β-catenin signaling pathway. *Biochemical and biophysical research communications.* 2016;477(4):749-754.

7. Yamashita S, Miyaki S, Kato Y, et al. L-Sox5 and Sox6 proteins enhance chondrogenic miR-140 microRNA expression by strengthening dimeric Sox9 activity. *The Journal of biological chemistry.* 2012;287(26):22206-22215.
8. Miyaki S, Nakasa T, Otsuki S, et al. MicroRNA-140 is expressed in differentiated human articular chondrocytes and modulates interleukin-1 responses. *Arthritis and rheumatism.* 2009;60(9):2723-2730.
9. Nakamura A, Rampersaud Y, Nakamura S, et al. microRNA-181a-5p antisense oligonucleotides attenuate osteoarthritis in facet and knee joints. *Annals of the rheumatic diseases.* 2019;78(1):111-121.
10. Wu J, Yang F, Wu X, Liu X, Zheng D. Comparison of genome-wide DNA methylation patterns between antler precartilage and cartilage. *Molecular Genetics and Genomics : MGG.* 2023;298(2):343-352.
11. Yang X, Yip J, Harrison M, Brockhausen I. Primary human osteoblasts and bone cancer cells as models to study glycodynamics in bone. *The International Journal of Biochemistry & Cell Biology.* 2008;40(3):471-483.
12. Bartel DP. MicroRNAs: genomics, biogenesis, mechanism, and function. *Cell.* 2004;116(2):281-297.
13. Kalluri R, LeBleu V. The biology function and biomedical applications of exosomes. *Science (New York, NY).* 2020;367(6478).
14. Sun H, Hu S, Zhang Z, Lun J, Liao W, Zhang Z. Expression of exosomal microRNAs during chondrogenic differentiation of human bone mesenchymal stem cells. *Journal of Cellular Biochemistry.* 2019;120(1):171-181.
15. Ali SA, Peffers MJ, Ormseth MJ, Jurisica I, Kapoor M. The non-coding RNA interactome in joint health and disease. *Nature Reviews Rheumatology.* 2021;17(11):692-705.
16. Jiang Y, Zhang L, Tian H. MicroRNA-149 improves osteoarthritis via repression of VCAM-1 and inactivation of PI3K/AKT pathway. *Experimental Gerontology.* 2023;174:112103.
17. Zhao Z, Zhao S, Luo L, et al. miR-199b-5p-DDR1-ERK signalling axis suppresses prostate cancer metastasis via inhibiting epithelial-mesenchymal transition. *British Journal of Cancer.* 2021;124(5):982-994.
18. Zhang M, Yuan S, Sun H, Sun L, Zhou D, Yan J. miR-199b-5p promoted chondrogenic differentiation of C3H10T1/2 cells by regulating JAG1. *Journal of tissue engineering and regenerative medicine.* 2020;14(11):1618-1629.
19. Qu X, Chen Z, Fan D, et al. MiR-199b-5p inhibits osteogenic differentiation in ligamentum flavum cells by targeting JAG1 and modulating the Notch signalling pathway. *Journal of cellular and molecular medicine.* 2017;21(6):1159-1170.
20. Huang J, Zhao L, Fan Y, et al. The microRNAs miR-204 and miR-211 maintain joint homeostasis and protect against osteoarthritis progression. *Nature communications.* 2019;10(1):2876.
21. Lu Y, Liu Y, Wan F, Shi S, Tao R. CircSmg5 stimulates the osteogenic differentiation of bone marrow mesenchymal stem cells by targeting the miR-194-5p/Fzd6 axis and beta-catenin signaling. *Environmental toxicology.* 2022;37(3):593-602.
22. Peng F, He Q, Cheng C, Pan J. GCNT2 induces epithelial-mesenchymal transition and promotes migration and invasion in esophageal squamous cell carcinoma cells. *Cell biochemistry and function.* 2019;37(1):42-51.

23. Sherman BT, Hao M, Qiu J, et al. DAVID: a web server for functional enrichment analysis and functional annotation of gene lists (2021 update). *Nucleic Acids Research.* 2022.
24. Chen Y, Wang X. miRDB: an online database for prediction of functional microRNA targets. *Nucleic acids research.* 2020;48:D127-D131.
25. Dweep H, Sticht C, Pandey P, Gretz N. miRWalk--database: prediction of possible miRNA binding sites by "walking" the genes of three genomes. *Journal of biomedical informatics.* 2011;44(5):839-847.
26. Li J, Liu S, Zhou H, Qu L, Yang J. starBase v2.0: decoding miRNA-ceRNA, miRNA-ncRNA and protein-RNA interaction networks from large-scale CLIP-Seq data. *Nucleic acids research.* 2014;42:D92-97.
27. Karagkouni D, Paraskevopoulou M, Chatzopoulos S, et al. DIANA-TarBase v8: a decade-long collection of experimentally supported miRNA-gene interactions. *Nucleic acids research.* 2018;46:D239-D245.
28. Agarwal V, Bell G, Nam J, Bartel D. Predicting effective microRNA target sites in mammalian mRNAs. *eLife.* 2015;4.
29. Pitcher T, Sousa-Valente J, Malcangio M. The Monoiodoacetate Model of Osteoarthritis Pain in the Mouse. *Journal of visualized experiments : JoVE.* 2016(111).
30. Choi W-S, Lee G, Song W-H, et al. The CH25H-CYP7B1-RORα axis of cholesterol metabolism regulates osteoarthritis. *Nature.* 2019;566(7743):254-258.
31. Cheah M, Fawcett J, Andrews M. Assessment of Thermal Pain Sensation in Rats and Mice Using the Hargreaves Test. *Bio-protocol.* 2017;7(16).
32. Glasson S, Chambers M, Van Den Berg W, Little C. The OARSI histopathology initiative - recommendations for histological assessments of osteoarthritis in the mouse. *Osteoarthritis and cartilage.* 2010:S17-23.

## Figure Legends

**Figure 1** MiRNA expression in KOA patients. **(A, B)** Volcano plot and heatmap showing differential miRNAs between KOA and healthy groups (healthy, $n$ = 10; KOA, $n$ = 15, $|\log2 \text{ Fold Change}| \geq 0.585$, $P < 0.05$). **(C)** GO and KEGG enrichment analyses of upregulated genes. **(D)** GO and KEGG enrichment analyses of downregulated genes.

**Figure 2** Verification with GEO data and miRNA screening. **(A, B)** Venn plot showing GEO dataset and our result. **(C)** RT-qPCR in clinical samples to verify the expression (HC, $n$ = 5, KOA, n = 5). **(D)** RT-qPCR results of mouse joint samples ($n$ = 6). Data are shown as means ± SD. *$P$<0.05, **$P$<0.01.

488 **Figure 3** Chondrocyte proliferation and marker expression changes after miR-199b-5p mimic
489 or inhibitor treatment. **(A)** Second generation primary mouse chondrocytes. **(B)** Toluene blue
490 staining. **(C)** Type II collagen immunoassay. **(D)** CCK-8 assay for cell viability (*n*=6). **(E, F)**
491 RT-qPCR detection of *MMP-3* and *ADAMTS5* mRNA expression (*n*=3). **(G-I)** RT-qPCR detec-
492 tion of *COL-2A1*, *AGGRECAN*, and *SOX9* mRNA expression (*n*=3). **(J)** CCK-8 cell viability
493 assay after different doses of LPS induction (*n*=5). **(K)** CCK-8 cell viability assay after virus in-
494 fection (*n*=6). **(L, M)** RT-qPCR detection of *MMP-3* and *ADAMTS5* mRNA expression (*n*=3).
495 **(N-P)** RT-qPCR detection of *COL2A1*, *AGGRECAN*, and *SOX9* mRNA expression (*n*=3). Data
496 are shown as means ± SD. **P*<0.05, ***P*<0.01.

497 **Figure 4** Injection of adenovirus expressing miR-199b-5p mimic results in inflammation and
498 pain threshold sensitivity in mice. **(A)** Animal experiment schematic. **(B)** Behavioral detection of
499 animal thermal pain threshold. **(C, D)** Detection of serum levels of *IFN-γ* and *TNF-α* in controls
500 by ELISA. **(E, F)** Safranin-fast green staining and semiquantitative scoring of articular cartilage.
501 **(G)** 3D reconstruction and 2D images of joints from μCT scans. Data are shown as mean ± SD.
502 **P*<0.05, ***P*<0.01, *n*=6.

503 **Figure 5** Injection of adenovirus expressing miR-199b-5p inhibitor partly recovered pathologi-
504 cal changes in KOA mice. **(A)** Animal experiment schematic. **(B)** Behavioral detection of animal
505 thermal pain threshold. **(C, D)** Detection of serum levels of *IFN-γ* and *TNF-α* in controls by
506 ELISA. **(E, F)** Safranin-fast green staining and semiquantitative scoring of articular cartilage.
507 **(G)** 3D reconstruction and 2D images of joints from μCT scans. Data are shown as mean ± SD.
508 **P*<0.05, ***P*<0.01, *n*=6.

509 **Figure 6** Validation of the miR-199b-5p target gene. **(A)** Prediction of target genes of miR-
510 199b-5p using search sites. **(B)** Target gene GO analysis. **(C, D)** Detection of the expression of

511 target genes under different conditions (*n*=3). **(E, F)** Predicting the binding site of miR-199b-5p
512 and target genes. **(G, H)** Validation by luciferase reporter gene assay (n=3). Data are show as
513 mean ± SD.**P*<0.05, ***P*<0.01, *n*=6. **(I-L)** The expression of FZD6 and GCNT2 in the synovial
514 membrane and chondrocytes of GEO Profiles KOA.

515 **Figure 7** miR-199b-5p exerts its effects on in vitro cells and in vivo mice by targeting *Fzd6* and
516 *Gcnt2*.

1 **Supplement table 1: Primer List**

| gene | sequence |
|---|---|
| U6 | GSP:5’GCTTCGGCAGCACATATACTAAAAT3’ |
| | R:5’CGCTTCACGAATTTGCGTGTCAT3’ |
| hsa-miR-199b-5p | GSP:5’GGGACCCCAGTGTTTAGACTAT3’ |
| | R: 5'GTGCGTGTCGTGGAGTCG3’ |
| hsa-miR-338-3p | GSP:5'GGGGGTCCAGCATCAGTGA3’ |
| | R:5’GTGCGTGTCGTGGAGTCG3’ |
| hsa-miR-15b-3p | GSP:5'GGGGCGAATCATTATTTGCT3’ |
| | R:5’ GTGCGTGTCGTGGAGTCG3’ |
| hsa-miR-1296-5p | GSP:5’GGTATTAGGGCCCTGGCTC3’ |
| | R:5’GTGCGTGTCGTGGAGTCG3’ |
| hsa-miR-3168 | GSP:5’TTGGGGGGGAGTTCTACAG3’ |
| | R:5’GTGCGTGTCGTGGAGTCG3’ |
| mmu-miR-199b-5p | GSP:5’GGGACCCCAGTGTTTAGACTAT3’ |
| | R: 5'GTGCGTGTCGTGGAGTCG3’ |
| mmu-miR-15b-3p | GSP:5'GGGGCGAATCATTATTTGCT3’ |
| | R:5’ GTGCGTGTCGTGGAGTCG3 |
| mmu-miR-338-3p | GSP:5'GGGGGTCCAGCATCAGTGA3’ |
| | R:5’GTGCGTGTCGTGGAGTCG3’ |
| Gapdh | F: TGTTTCCTCGTCCCGTAGA |
| | R: ATCTCCACTTTGCCACTGC |
| Hif-1α | F: GGGGAGGACGATGAACATCAA |
| | R: GGGTGGTTTCTTGTACCCACA |
| Fzd6 | F: AGAGGTGAAAGCGGACGGA |
| | R: AGAGAGTCTGGAGATGGATGCT |
| Gcnt2 | F: TCCTGGACGGGTAACCTCAG |
| | R: CTGCAAGTCTCCGTTTCCATAG |
| Myh9 | F: AGAAGTTGGTATGGGTGCCTT |
| | R: CCCTGAGTAGTATCGCTCCTTG |
| Caprin1 | F: GAAGCAGATTCTCGGCGTAAT |
| | R: TCCCCTTTATTCATTCGTTCCTG |
| Atg14 | F: GAGGGCCTTTACGTGGCTG |
| | R: AATAGACGAAATCACCGCTCTG |
| Mmp3 | F: ACTGTGTCCCAAGGAGAGGAG |
| | R: AAACCATCTACACAGTTCAGACAC |
| Adamts5 | F: ATGCAGCCATCCTGTTCACC |
| | R: AAGGCCAAGTAGATGCCCAATTT |
| Aggrecan | F: CACTGTCAAAGCACCATGCC |
| | R: TAGGCTGGCTCCCATTCAGT |

| | |
|---|---|
| Sox9 | F: TAATTCCCCAGGCTCTTGGAT |
| | R: GCAGCCGGGATTTAAGGCTC |
| Col2a1 | F: CACGCATGAGCCGAAGCTA |
| | R: GGGTTTCCACGTCTCACCA |

**Supplement table 2: Basic information for recruiting patients**

| **Baseline** | **KOA（N=15）** | **HC（N=10）** | ***P* value** |
|---|---|---|---|
| Age | 52.67 ± 7.35 | 51.50 ± 7.71 | 0.706 |
| Height | 1.63±0.07 | 1.60±0.05 | 0.201 |
| Weight | 65.03±9.53 | 61.30±8.47 | 0.327 |
| BMI | 24.28 ± 2.39 | 23.90± 2.65 | 0.715 |

**Fig 1**

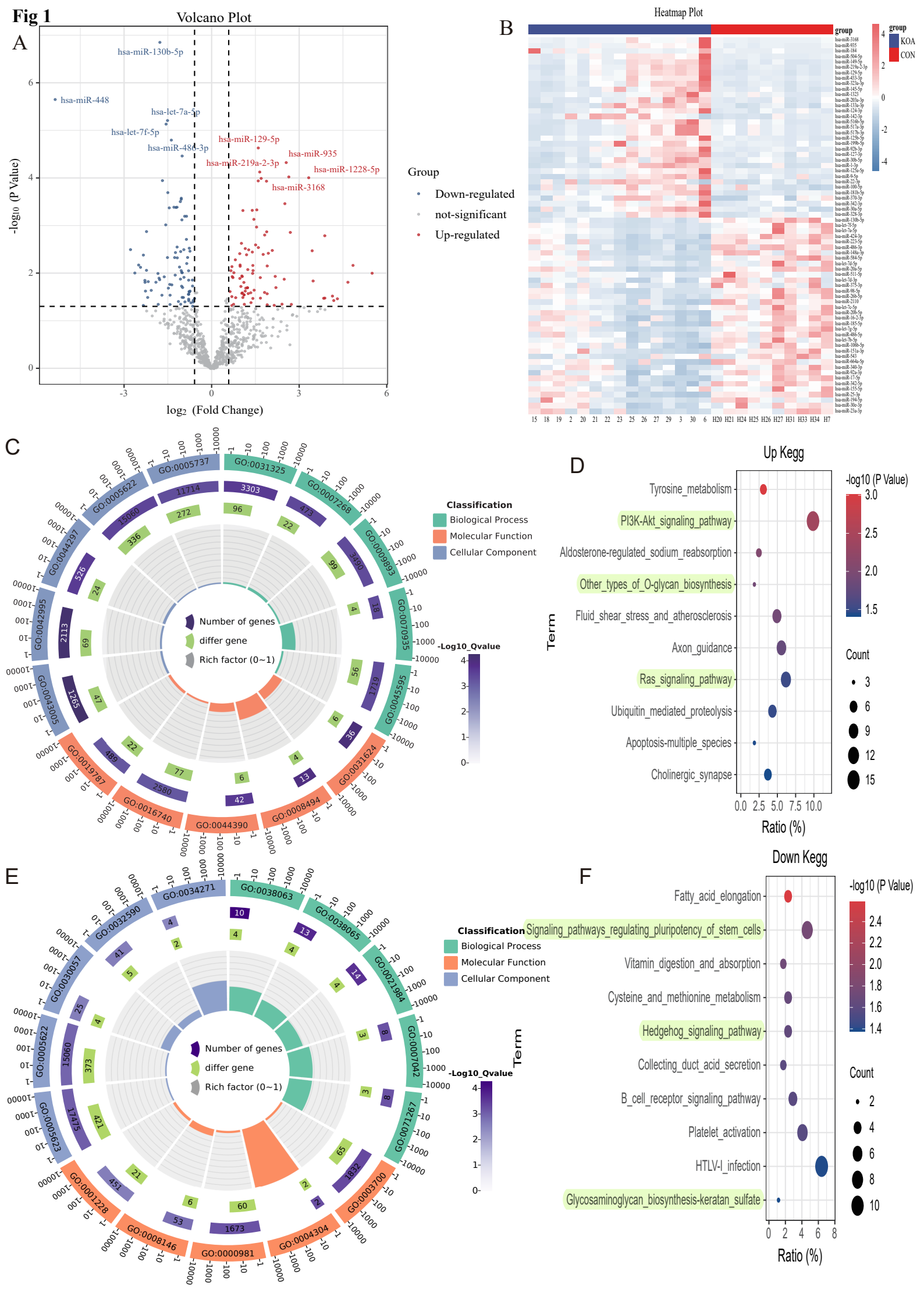
A
Volcano Plot
hsa-miR-130b-5p
hsa-miR-448
hsa-let-7a-5p
hsa-let-7f-5p
hsa-miR-486-3p
hsa-miR-129-5p
hsa-miR-935
hsa-miR-219a-2-3p
hsa-miR-1228-5p
hsa-miR-3168
-log10 (P Value)
log2 (Fold Change)
Group
Down-regulated
not-significant
Up-regulated
B
Heatmap Plot
group
KOA
CON
C
Classification
Biological Process
Molecular Function
Cellular Component
Number of genes
differ gene
Rich factor (0~1)
-Log10_Qvalue
D
Up Kegg
Tyrosine_metabolism
PI3K-Akt_signaling_pathway
Aldosterone-regulated_sodium_reabsorption
Other_types_of_O-glycan_biosynthesis
Fluid_shear_stress_and_atherosclerosis
Axon_guidance
Ras_signaling_pathway
Ubiquitin_mediated_proteolysis
Apoptosis-multiple_species
Cholinergic_synapse
Term
Ratio (%)
-log10 (P Value)
Count
E
Classification
Biological Process
Molecular Function
Cellular Component
Number of genes
differ gene
Rich factor (0~1)
-Log10_Qvalue
F
Down Kegg
Fatty_acid_elongation
Signaling_pathways_regulating_pluripotency_of_stem_cells
Vitamin_digestion_and_absorption
Cysteine_and_methionine_metabolism
Hedgehog_signaling_pathway
Collecting_duct_acid_secretion
B_cell_receptor_signaling_pathway
Platelet_activation
HTLV-I_infection
Glycosaminoglycan_biosynthesis-keratan_sulfate
Term
Ratio (%)
-log10 (P Value)
Count

**Fig 2**

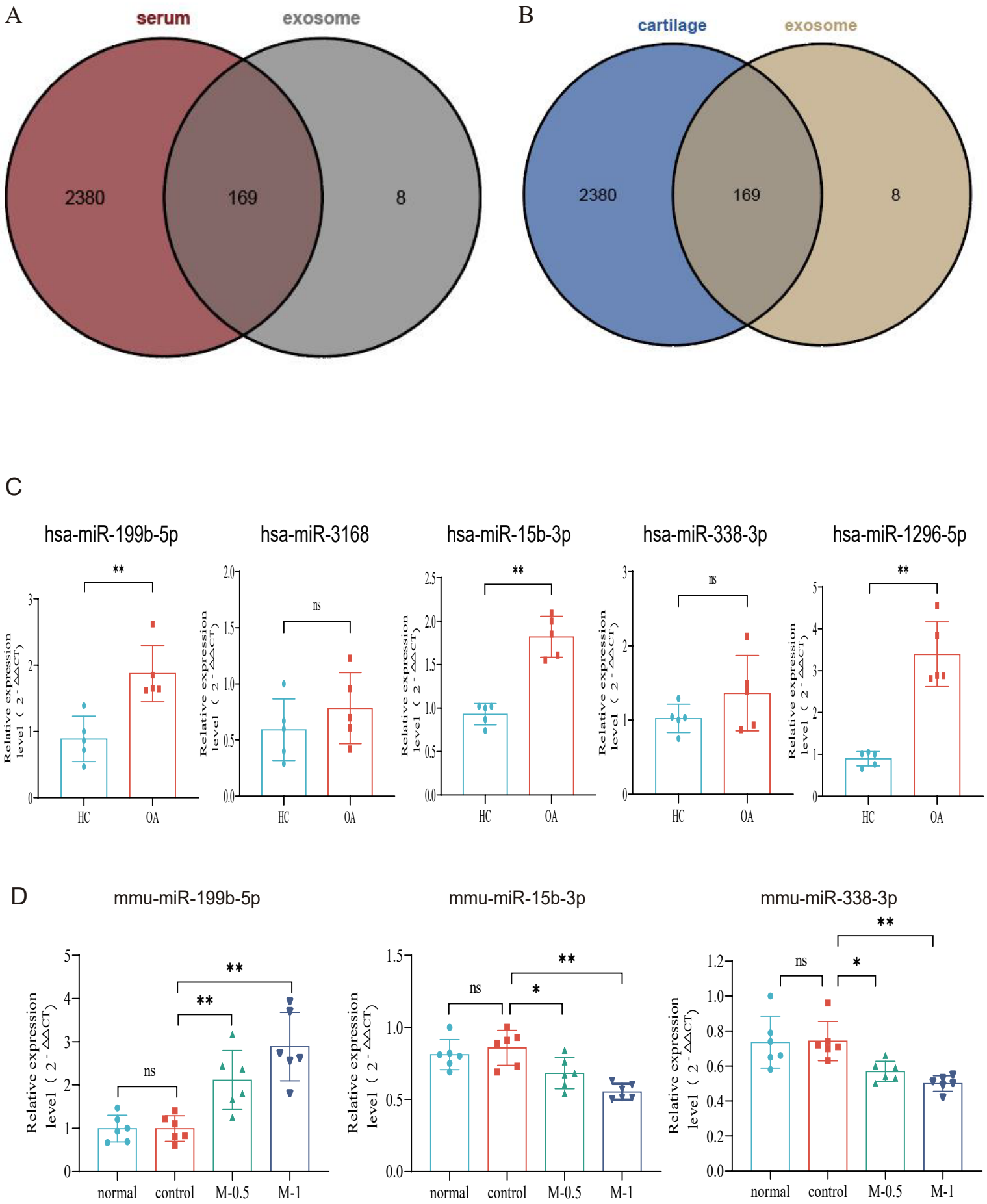
A
serum
exosome
2380
169
8
B
cartilage
exosome
2380
169
8
C
hsa-miR-199b-5p
hsa-miR-3168
hsa-miR-15b-3p
hsa-miR-338-3p
hsa-miR-1296-5p
Relative expression level（2-△△CT）
HC
OA
**
ns
D
mmu-miR-199b-5p
mmu-miR-15b-3p
mmu-miR-338-3p
normal
control
M-0.5
M-1
ns
*
**

Fig 3

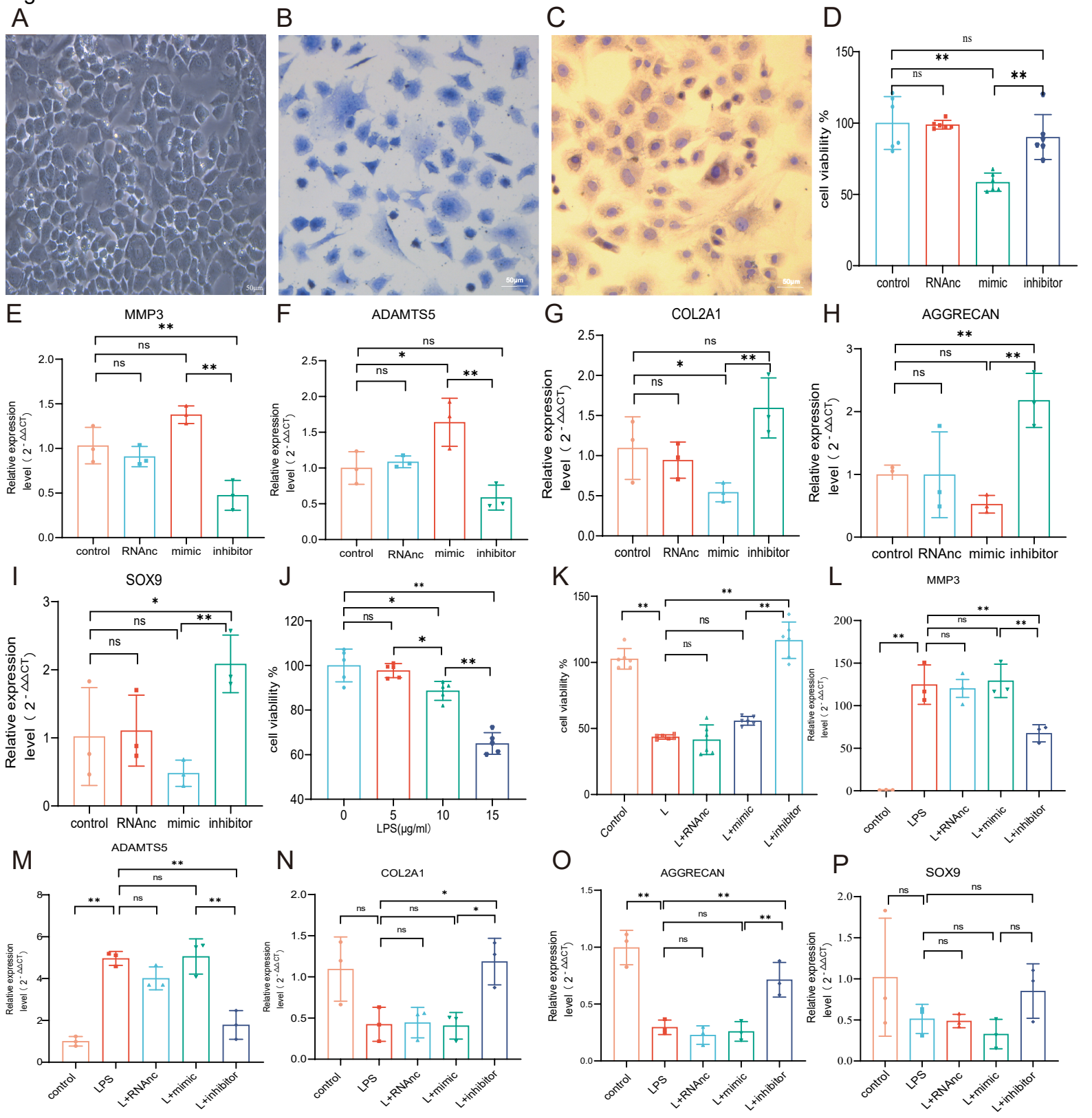
A
B
C
D
cell viability %
control
RNAnc
mimic
inhibitor
E
MMP3
F
ADAMTS5
G
COL2A1
H
AGGRECAN
Relative expression level ( 2 - ΔΔCT)
I
SOX9
J
cell viability %
LPS(μg/ml)
K
cell viability %
Control
L
L+RNAnc
L+mimic
L+inhibitor
L
MMP3
LPS
M
ADAMTS5
N
COL2A1
O
AGGRECAN
P
SOX9

**Fig 4**

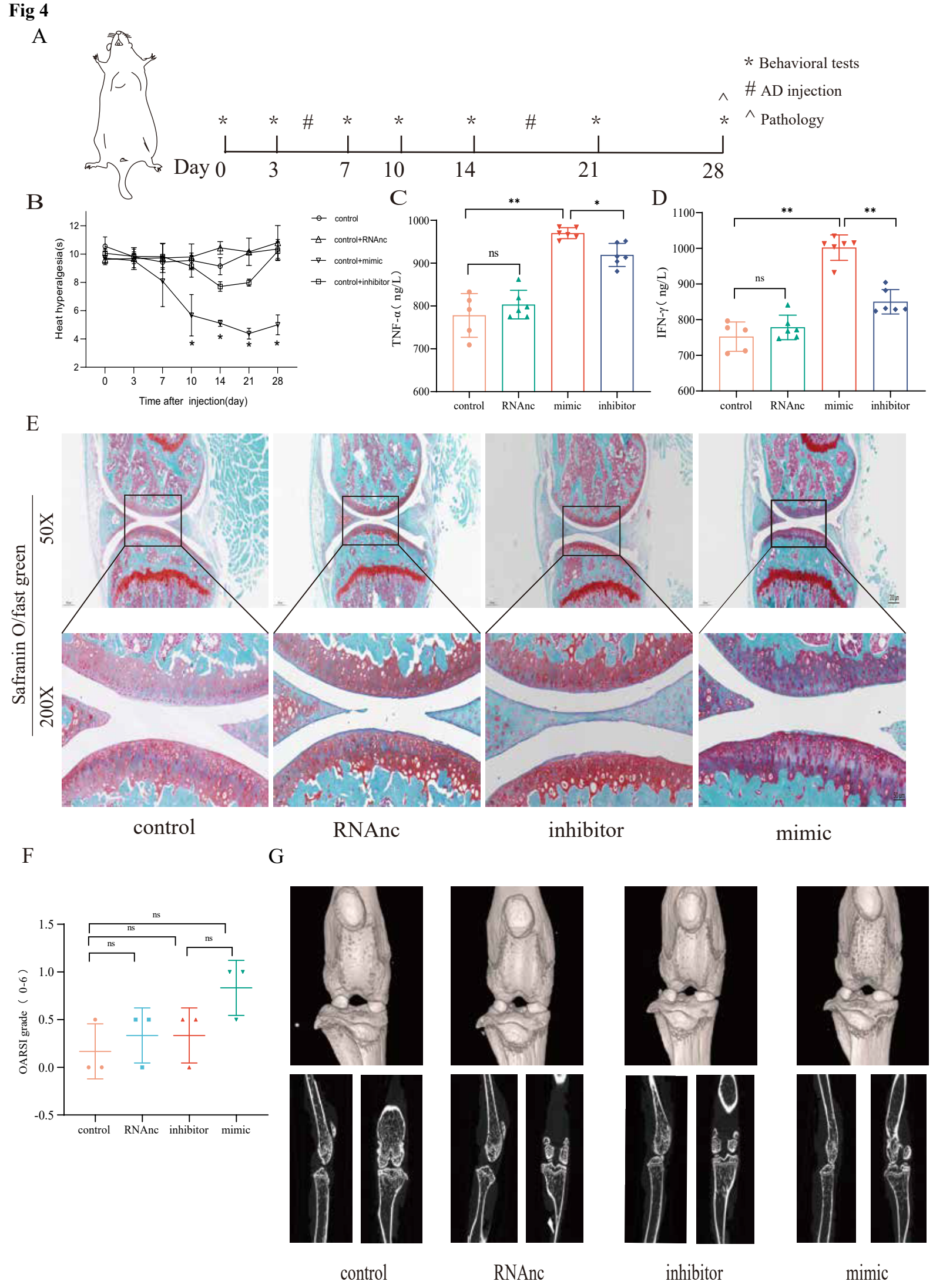
A
* Behavioral tests
# AD injection
^ Pathology
Day 0 3 7 10 14 21 28
B
Heat hyperalgesia(s)
Time after injection(day)
control
control+RNAnc
control+mimic
control+inhibitor
C
TNF-α（ng/L）
ns
control
RNAnc
mimic
inhibitor
D
IFN-γ（ng/L）
E
Safranin O/fast green
50X
200X
control
RNAnc
inhibitor
mimic
F
OARSI grade（0-6）
ns
control
RNAnc
inhibitor
mimic
G
control
RNAnc
inhibitor
mimic

**Fig 5**

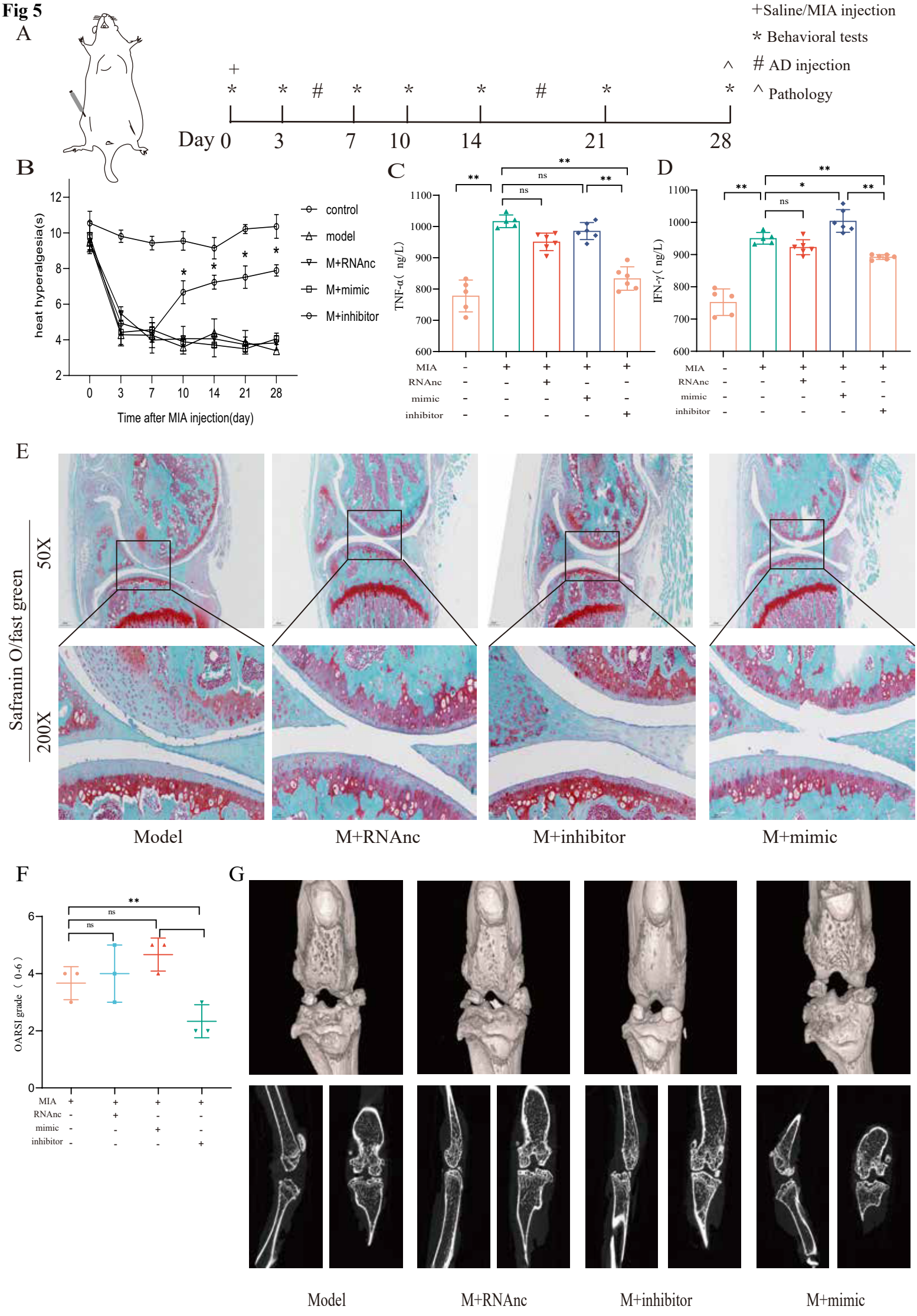
A
+Saline/MIA injection
* Behavioral tests
# AD injection
^ Pathology
Day 0 3 7 10 14 21 28
B
heat hyperalgesia(s)
Time after MIA injection(day)
control
model
M+RNAnc
M+mimic
M+inhibitor
C
TNF-α ( ng/L)
D
IFN-γ ( ng/L)
MIA
RNAnc
mimic
inhibitor
E
Safranin O/fast green
50X
200X
Model
M+RNAnc
M+inhibitor
M+mimic
F
OARSI grade ( 0-6 )
G
Model
M+RNAnc
M+inhibitor
M+mimic

Fig 6

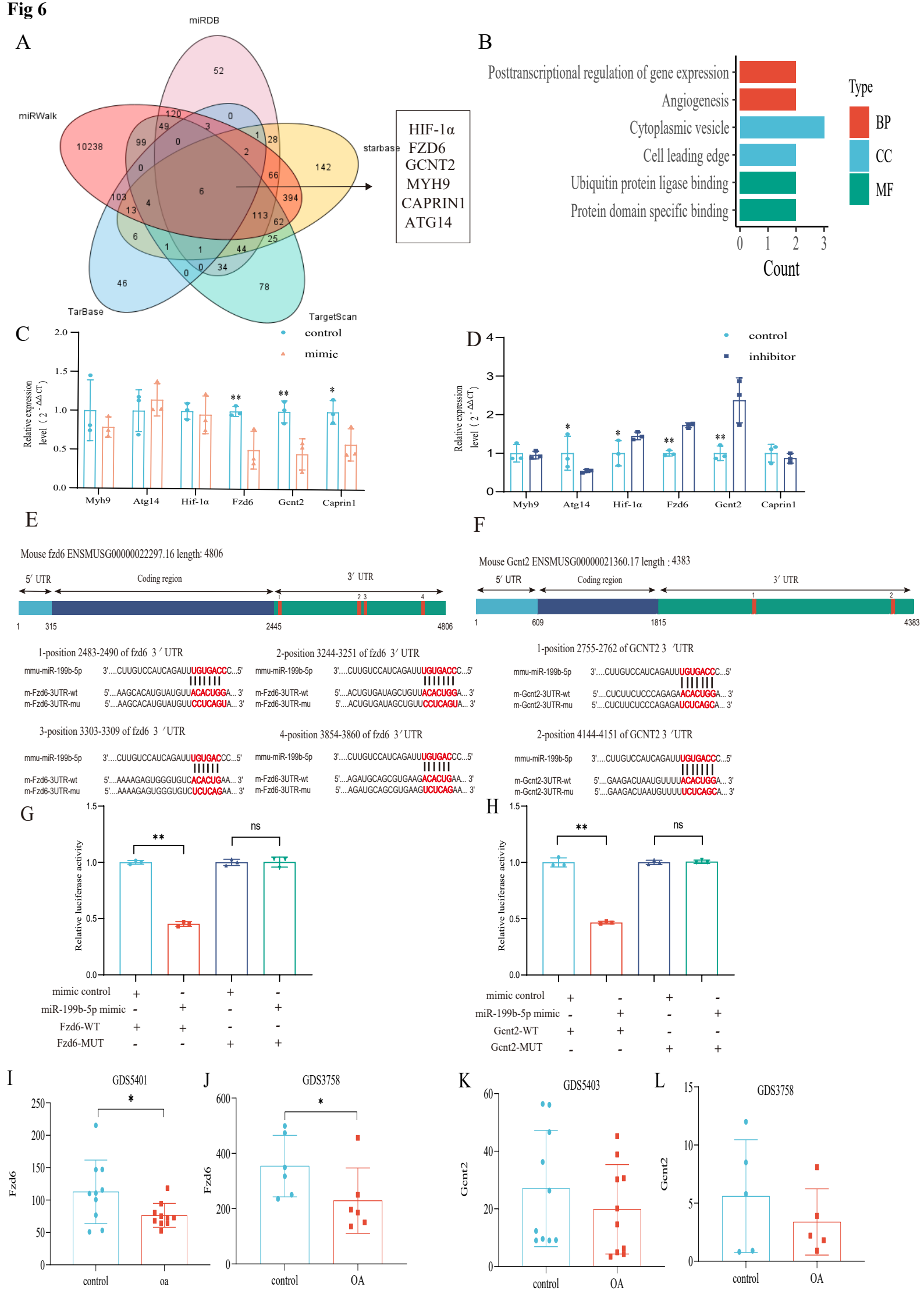

A
miRDB
miRWalk
starbase
TarBase
TargetScan
HIF-1α
FZD6
GCNT2
MYH9
CAPRIN1
ATG14
B
Posttranscriptional regulation of gene expression
Angiogenesis
Cytoplasmic vesicle
Cell leading edge
Ubiquitin protein ligase binding
Protein domain specific binding
Type
BP
CC
MF
Count
C
control
mimic
Relative expression level ( 2 - ΔΔCT)
Myh9
Atg14
Hif-1α
Fzd6
Gcnt2
Caprin1
D
control
inhibitor
E
Mouse fzd6 ENSMUSG00000022297.16 length: 4806
5′ UTR
Coding region
3′ UTR
1-position 2483-2490 of fzd6 3′UTR
2-position 3244-3251 of fzd6 3′UTR
3-position 3303-3309 of fzd6 3′UTR
4-position 3854-3860 of fzd6 3′UTR
mmu-miR-199b-5p
m-Fzd6-3UTR-wt
m-Fzd6-3UTR-mu
F
Mouse Gcnt2 ENSMUSG00000021360.17 length : 4383
1-position 2755-2762 of GCNT2 3′UTR
2-position 4144-4151 of GCNT2 3′UTR
m-Gcnt2-3UTR-wt
m-Gcnt2-3UTR-mu
G
Relative luciferase activity
ns
mimic control
miR-199b-5p mimic
Fzd6-WT
Fzd6-MUT
H
Gcnt2-WT
Gcnt2-MUT
I
GDS5401
Fzd6
control
oa
J
GDS3758
OA
K
GDS5403
Gcnt2
L

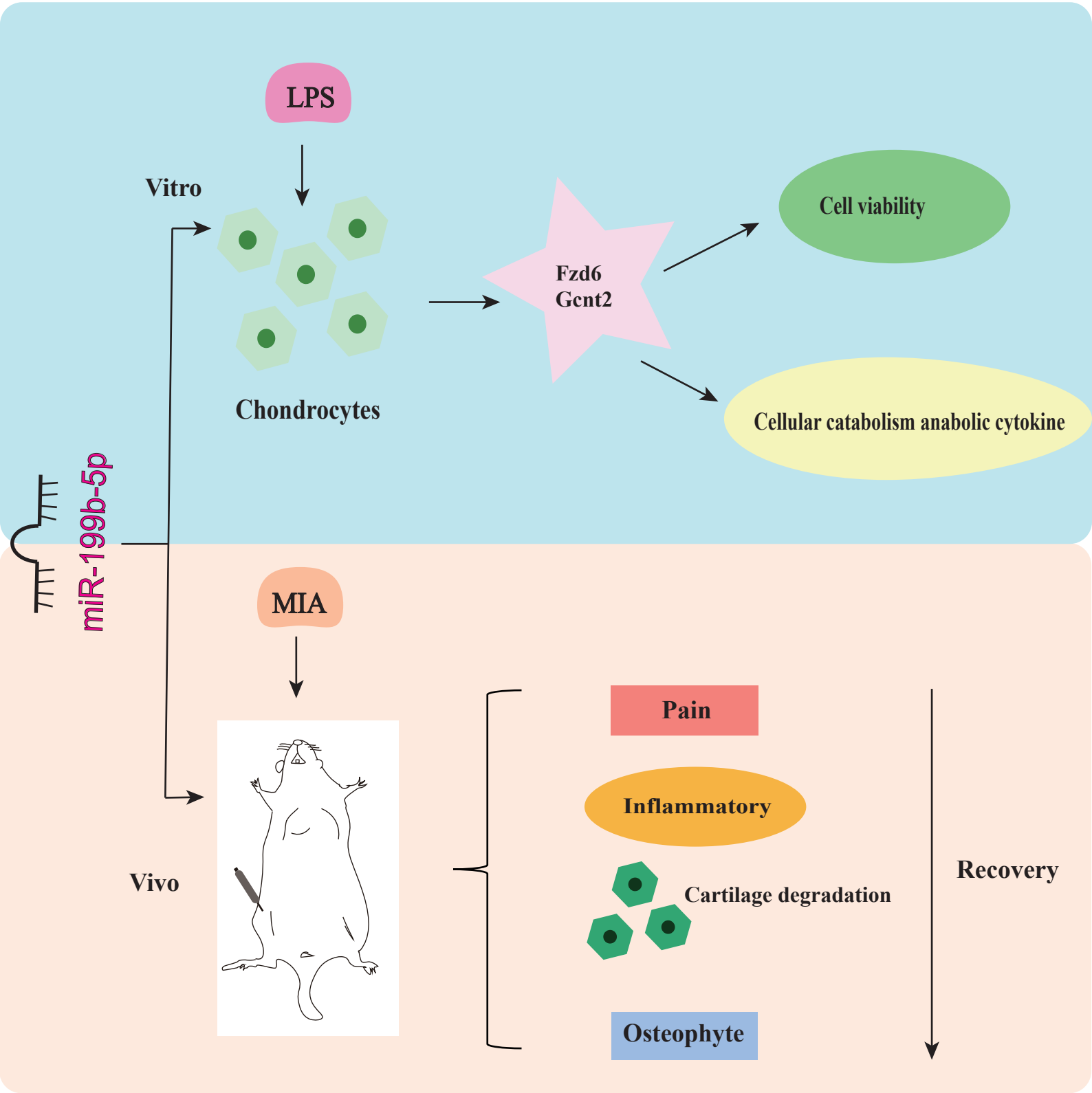
LPS
Vitro
Chondrocytes
Fzd6
Gcnt2
Cell viability
Cellular catabolism anabolic cytokine
miR-199b-5p
MIA
Vivo
Pain
Inflammatory
Cartilage degradation
Osteophyte
Recovery